



# Heuristic urban transportation network design method, a multilayer coevolution approach



Rui Ding<sup>a</sup>, Norsidah Ujang<sup>a</sup>, Hussain bin Hamid<sup>b</sup>,  
Mohd Shahrudin Abd Manan<sup>a</sup>, Rong Li<sup>c</sup>, Jianjun Wu<sup>c,\*</sup>

<sup>a</sup> Faculty of Design and Architecture, Universiti Putra Malaysia, Serdang, 43400 Selangor, Malaysia

<sup>b</sup> Faculty of Engineering, Universiti Putra Malaysia, Serdang, 43400 Selangor, Malaysia

<sup>c</sup> State Key Laboratory of Rail Traffic Control and Safety, Beijing Jiaotong University, 100044 Beijing, China

## HIGHLIGHTS

- A multilayer urban network co-evolution approach is proposed.
- The relative neighbourhood graph (RNG) and Gabriel graph (GG) are used to simulate the structure of upper and lower networks, respectively.
- The cooperation strength and operation speed ratio are considered in depth in different layers and in impact of the user behaviour on the change of network structures.

## ARTICLE INFO

### Article history:

Received 27 November 2016

Received in revised form 15 February 2017

Available online 28 February 2017

### Keywords:

Complex network  
Urban transportation  
Network design  
Coevolution approach  
Multilayer network

## ABSTRACT

The design of urban transportation networks plays a key role in the urban planning process, and the coevolution of urban networks has recently garnered significant attention in literature. However, most of these recent articles are based on networks that are essentially planar. In this research, we propose a heuristic multilayer urban network coevolution model with lower layer network and upper layer network that are associated with growth and stimulate one another. We first use the relative neighbourhood graph and the Gabriel graph to simulate the structure of rail and road networks, respectively. With simulation we find that when a specific number of nodes are added, the total travel cost ratio between an expanded network and the initial lower layer network has the lowest value. The cooperation strength  $\lambda$  and the changeable parameter average operation speed ratio  $\theta$  show that transit users' route choices change dramatically through the coevolution process and that their decisions, in turn, affect the multilayer network structure. We also note that the simulated relation between the Gini coefficient of the betweenness centrality,  $\theta$  and  $\lambda$  have an optimal point for network design. This research could inspire the analysis of urban network topology features and the assessment of urban growth trends.

© 2017 Elsevier B.V. All rights reserved.

## 1. Introduction

Studies of urban transportation networks have significant implications for urban policies and private investment and are generally important in the urban planning chain. In addition to transport planners and engineers, there is a distinguished

\* Corresponding author.

E-mail address: [jjwu1@bjtu.edu.cn](mailto:jjwu1@bjtu.edu.cn) (J. Wu).

tradition of architects, urban designers, planners and landscape architects who have recognized the significance of transport for structuring cities. This recognition is particularly undeniable in the modernist era in which transportation efficiency is considered as one of the 'prime shaper of urban space' and the reflection of traffic flow is the direct representation of the quality of traffic network design and optimization. The transportation network plays a vital role in regions and societies, research on the transportation network and topological structure characteristics provides relevant references for transportation network planning, design and maintenance [1–6].

Meanwhile, more people are clustering closer together in finite and large metropolitan areas in which growing populations are accompanied by increasing traffic. Population distribution is the most frequently considered mechanism and is shown to have the most significant effect on the evolution of urban road network, and in some points, the influence of population growth can be treated as the most important driving factors during the urban sprawl process [7,8]. However, the network evolution studies normally ignore the influence of population growth [9]. Hence we believe that it has an enormous potential for further discussion.

Analysing and modelling the evolution of transportation networks has been a subject of scholarly interest for more than 50 years, with the relevant studies tracking the following research streams. Based on the foregoing, evolutionary studies of urban networks have garnered more attention recently, as researchers have mainly considered the traditional effects of the structure of subway networks, the evolutionary process of urban networks and the robustness of these networks. The effects of network evolution include the influence of nearby nodes on traffic diversion, costs in terms of time, the push of local populations and surrounding land prices [8,10–13]. Barthélemy and Flammini [14] used the optimization principles of traffic networks to propose a spanning tree simulation model, in which tree structures change with their defined numerical value parameters. Whether or not the studies consider the spatial constraints, some critical qualitative features of these networks can be imitated using the simulated optimized network structures by varying only one parameter in the cost function. Levinson & Yerra demonstrated a travel demand model coupled with revenue, cost and investment models of a grid network to investigate the self-organization of surface transportation networks [15,16], they showed that a transportation network with a fixed structure can be distinguished as a random or a uniform state, and they revealed that roads and hierarchies, which are often thought to be the products of conscious design, can also be self-organized. Gao, Sun, Wu et al. investigated and analysed an optimal traffic network structure for resisting traffic congestion featuring different volumes of traffic, they introduced a cost function and user equilibrium (UE) assignment that ensured the flow balance of traffic systems and expanded both the bi-level programming model and its solution algorithms [17–19]. However, most of related research has disregarded the continuous interaction between decision-makers, suppliers and users with independent interests, which is critical for determining and shaping the fundamental structure of transportation networks.

Other researchers have noted the importance and advantages of coevolution models. Focusing on the coevolution model of population distribution, land use and the transportation network of the 19th and 20th century London, Levinson and Xie found that population density and network density are positively correlated. They validated a simulation model to better fit the empirical evidence and noted that evolution is an iterative process of interaction, investment and divestment. Moreover, they illustrated how surface transportation networks can grow and decline spontaneously over time, providing further evidence for the property of self-organization [20–23]. The coevolution of road expansion and urban traffic growth grounded on the case of Beijing is described [24], and a coevolution model is suggested, conducting a stability analysis and numerical simulation. Subsequently, Li, Wu [25] proposed an integrated coevolution general bi-level programming model of land use and traffic network design. They analysed and simulated the relationship between two types of economic agents – government investment decisions vs. household and company locations – to show that average accessibility for employment and population rises in the evolution process. Ding, Ujang [26] suggested that constrained measures of general network efficiency should be considered as another effect. Based on a network topological structure and related indices, the effects of four typical growth styles were considered, revealing that different strategies have uneven effects on network optimization and the growth process. Zhao et al. built on the research of Levinson et al. and revealed the interactions between population distribution and urban road network evolution based on simulation models. Using a relative neighbourhood graph (RNG) and a Fermat–Weber location problem as the connection mechanism, these authors revealed that the population distribution in a city is the leading cause of heterogeneity in a network topology structure [27–29]. Given the evolution of urban form, the most intuitive parts of the urban system are the divisions of the highway and railway networks, followed by the intensive forms of building representation. From the perspective of economics and land use, building density is determined by population distribution [30,31]. Therefore, the ternary structure of urban form (roads, intersections and buildings) can be converted into the relationship between the road system and the population distribution.

Although these previous researches are important and necessary, they do not consider the influence of multilayer networks, which illustrate and represent different appropriate urban traffic modes. Development of rail and road networks is inseparable from the development of a prosperous urban area; thus, research on multilayer networks has scientific potential and fulfils a real need. To bridge the gap of the multilayer network representation of real world networks Kurant and Thiran [32] first proposed a general multilayer model that facilitated the description and analysis of multilayer networks. These authors examined three transportation networks and found that a tiny error on a multilayer network could cause disaster. They also investigated the relationship between degree, betweenness and real loads and found that, as opposed to the commonly acknowledged view, the correlations in their data set between the three factors were not that apparent. Later, Buldyrev, Parshani [33] demonstrated that electrical blackout results in the cascading failure of the Internet communication network and power stations in Italy. Their research serves as the breakthrough milestone in the

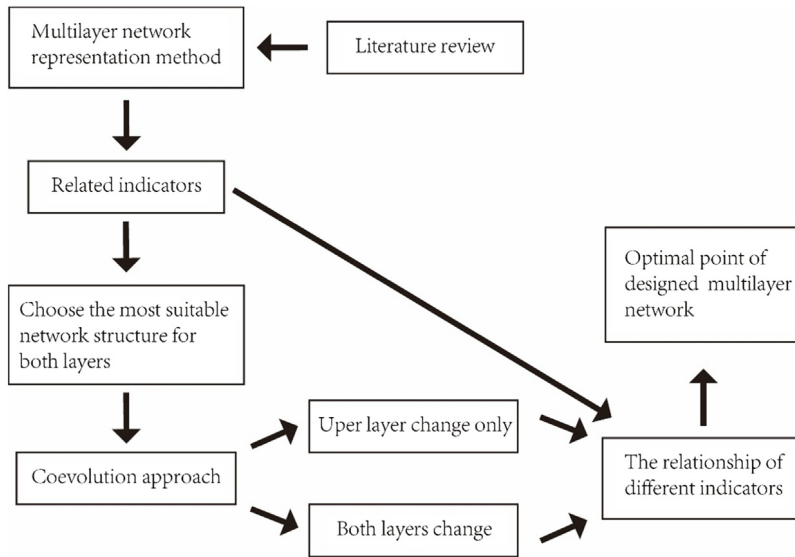


Fig. 1. The framework of this paper.

measurement of interactions in layered networks. These authors deciphered the critical percolation threshold, which is larger than the equivalent threshold of a single-layer network of the same size. More recently, multilayer networks earned a lot of attentions, traffic dynamics on two-layer complex networks were considered by Ma, Han [34–36], and Solé-Ribalta, Gómez [37] introduced a standardized model to simulate the elements navigating those networks and analysed congestion in multilayer transportation networks. Most outstandingly, a model of traffic dynamics and revealed a transition at the onset of cooperation between layered networks is proposed by Gu, Zou [38]; they introduced the notion of the cooperation strength of different layers to illuminate the relation of coupling networks. Additionally, Strano, Shai [13] considered the impact of the multilayer structure of the street network and the subway system based on the change of shortest path length and noted that undesired uneven spatial distributions of accessibility might be triggered by the increasing of subway speed. These researchers investigated the aspects of multilayer networks to consider the interrelationship and cooperation of different traffic models.

This article employs the understanding of multilayer network concepts to analyse the relationship between railway and traffic networks and their laws of coevolution, and population distribution is considered and have the most significant effect on the coevolution process. It demonstration that general network design is highly related to the network cooperation strength and future operation speed ratio of different layers and that the maintenance and the better operation of the existing networks also rely on these indicators, and critical and meaningful for the network design.

Temporarily we do not consider other factors such as the economy, and we not discuss the induced demand here, which make the calculation and discussion far more complex and not in line with our research aim, so we will leave them to our further research. The next section give the materials and methods used by this study, illustrated the multilayer network representation method, the network coevolution model and related hypothesis. Then section four reveals novel characteristics of multilayer networks based on the simulation of network corresponding evolution process and analyses the results. Section five provides conclusions and proposes future research directions. We shown the structure of this paper as a flowchart (Fig. 1) to make it can be understood easily and clearly.

## 2. Materials and methods

### 2.1. Multilayer network representation method

The multilayer representation method is defined as M-space, similar to the definition of L-space [39] and P-space [40] – or the primal and dual approach, respectively – which were initially proposed by S. Porta, P. Crucitti and V. Latora. Accordingly, we simply refer to the general urban transportation system as a multilayer network. In our models, the upper layer network represents the public rail network, which may include rapid transit, LRT, Monorail, MRT and subway; here, we do not distinguish among rail transit modes. The lower layer network represents the urban traffic networks, which are the road network topology or OD zones (urban network communities). Then we use the widely accepted basic graph theory and complex and multilayer network theory representation methods to represent them. The undirected multilayer network can be represented as  $G = \langle G^U, G^L \rangle$  (see Fig. 2(a)), i.e., as the set of different layers; here, we use the superscript  $U$  to define the upper layer network and superscript  $L$  to set the lower layer [17,38]. The rail network and urban road network can be represented as connected network  $G^U = \langle V^U, E^U, W^U \rangle$  and  $G^L = \langle V^L, E^L, W^L \rangle$  in its primal weighted (denoted by

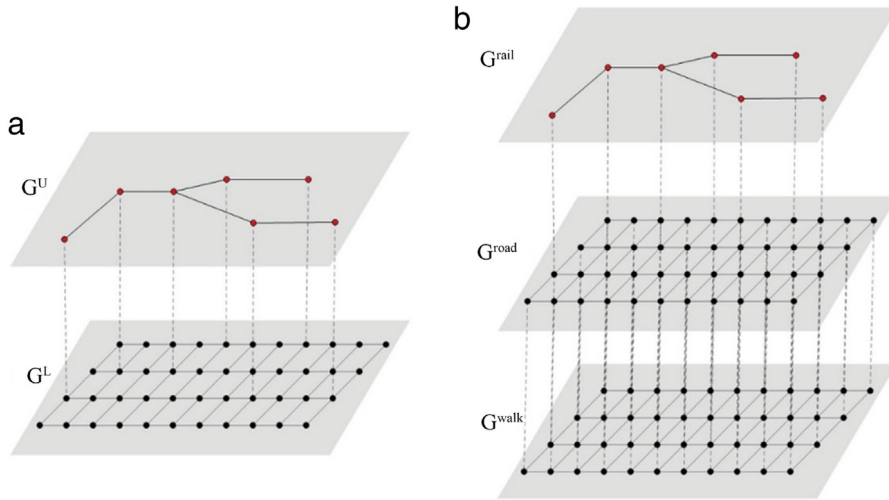


**Fig. 2.** (a) The multilayer network model of urban traffic networks; the upper layer represents rail network topology, and the lower layer represents the road network topology. (b) The multilayer network model can be expanded to represent multimodal transportation and their interrelations. (For interpretation of the references to colour in this figure legend, the reader is referred to the web version of this article.)

$W$  in function) representation [41]; red nodes represent rail stations and black nodes represent road intersections; solid lines represent their connections, and dotted lines represent crossing links (cooperative relationship) between different layers. This type of multilayer network can be easily extended to represent multimodal transportation and relations between the vehicle-based network and the pedestrian network (abbreviated as  $G^{walk}$ ) (see Fig. 2(b)). Because we normally design dissimilar levels of street paths for pedestrians and vehicles to fulfil their different transport needs, the coupled network relationships can be found between  $G^{road}$  and  $G^{walk}$ , respectively.

Moreover, in this definition,  $V$  is the set of the nodes in which  $N$  is the node number of lower layer when  $V = \{V_i | i \in I \equiv \{1, 2, \dots, N\}\}$ ,  $E$  represents the unordered pairs of edges and elements of  $V$  and is denoted by  $e_{ij}$ , and  $E = \{e_{ij} = (v_i, v_j) | i, j \in I\}$ ; similarly, we have the definition of multilayer network  $N^{multi} = N^U + N^L$ ,  $V^{multi} = V^U + V^L$ ,  $E^{multi} = E^U + E^L + E^C$ . The adjacency matrix of lower layer networks  $adj = [a_{ij}]_{n \times n}$  is symmetrical and non-negative, representing the connection between zones  $i$  and  $j$ , where  $a_{ij} = \begin{cases} d_{ij} \times W, & (v_i, v_j) \in E \\ 0, & (v_i, v_j) \notin E \end{cases}$ , where  $d_{ij}$  is the Euclidean distance. Define  $a_{ii} = 0$  to theoretically remove any self-connections; in reality, we do not consider the impact of the network element itself. Then, the adjacency matrix of multilayer networks is  $adj^{multi} = \begin{bmatrix} adj_{N^U \times N^U}^U & adj_{N^U \times N^L}^C \\ adj_{N^L \times N^U}^C & adj_{N^L \times N^L}^L \end{bmatrix}$ , which can reduce the network's spatial dimension.

## 2.2. Basic related indicators

Some basic definitions and theoretical analysis reviewed and proposed by Derrible and Kennedy [42], Morris and Barthélemy [43], Strano, Shai [13] and Ding, Ujang [26] are used with slight adjustments in this research.

Given two nodes,  $v_i, v_j \in V$ , let  $d_{min}^{ij}$  be the shortest path length (SPL) between them, considering the travel cost,  $d_{min}^{ij}$  will highly related with the average speed of different layers,  $D$  is the network diameter. The average shortest path length of the network is then described as:

$$APL = \frac{1}{N(N-1)} \sum_{i \neq j} d_{min}^{ij}, \quad (1)$$

and  $N$  is the total number of nodes. Regarding the efficiency of the global network,  $EG$  is the inverse of  $APL$  between each pair of nodes  $v_i$  and  $v_j$  and is computed as:

$$E(G) = \frac{1}{N(N-1)} \sum_{i \neq j} \frac{1}{d_{min}^{ij}}. \quad (2)$$

Closeness Centrality (CC) is denoted as the reciprocal of the average distance between each node pairs [44], as:

$$C_{closeness}(v_i) = \frac{1}{D_{ij}} = \frac{N-1}{\sum_{i \neq j} d_{ij}}. \quad (3)$$

This index describes the relative location and importance of a node, means that if a node is typically “close” to other nodes, it is more important in the network. Betweenness centrality (BC) is originally defined by Freeman [45] as the ratio between the total number of shortest paths between two separate nodes  $d_{min, st}$  and the shortest paths passing through a specific node  $d_{min, st}^i$ ; it reflects the load on node  $v_i$  and can alternately understand as the controllability of the node. In the research of modern urban traffic networks, betweenness centrality is an essential index; it also acted as the key point of Multiple Centrality Assessment (MCA) [46–50]. On this basis, centrality can be clarified as:

$$C_{betweenness}(v_i) = \sum_{i \neq s \neq t \in V} \frac{d_{min, st}^i}{d_{min, st}}, \quad (4)$$

and the normalization of betweenness is described as:

$$BC(v_i) = \frac{\sum_{i \neq s \neq t \in V} \frac{d_{min, st}^i}{d_{min, st}}}{(N-1)(N-2)}. \quad (5)$$

### 2.3. The indicators of multilayer traffic networks

In the multilayer network, we can easily observe the difference in transport operation speeds in the multimodal transportation system, as trains move faster than vehicles in a normal urban system. This gap makes the system user choose a balance of trip and transport modes to save travel cost (whether time, energy or money). To reflect this difference, a theoretically changeable parameter of average operation speed ratio similar to the theoretical analysis is proposed [43]:

$$\Theta = \frac{S^L}{S^U}, \quad 0 < \Theta < 1, \quad (6)$$

to address the ratio of speeds in different layers, where  $S^L$  and  $S^U$  are the average speeds of the lower layer and the upper layer, respectively. This parameter measures the general travel cost in time units associated with the with both layers. A smaller parameter value corresponds to a faster upper layer traverse speed and can be changed based on the various transport policies of different cities and their requirements.

The path with the smallest total weight between any two OD zones is called the shortest weighted paths. Also, the travel cost of the lower layer network's shortest weighted path can be defined as  $w_s \tau_s$ . Similarly, we have the travel expenses of the shortest weighted path of the rail network  $w_r \tau_r$ , and the travel costs on the shortest weighted path of crossing links  $w_c \tau_c$ , where  $w_s$ ,  $w_r$  and  $w_c$  are the weights of the related links on different layers, see Fig. 3(a).

We denote the total shortest weighted path distance of trips passing upper layer links, crossing links and lower layer links connecting zones  $i$  and  $j$  by  $U_{ij}$ ,  $C_{ij}$ , and  $L_{ij}$ , respectively. Therefore, cooperation strength can be defined as

$$\Lambda = \frac{1}{N(N-1)} \sum_{i \neq j} \frac{C_{ij}}{U_{ij} + L_{ij} + C_{ij}}, \quad (7)$$

when the value of  $\Lambda$  is smaller, cooperation is stronger. In other words, if the distance between zone  $i$  and zone  $j$  passing through intralayer links increases for some reason, users choose a more convenient mode of transportation, such as only using the lower layer network and giving up the rail network. In this case, there is no cooperation, which differs from the definition in Gu, Zou [38] and Strano, Shai [13]. The strength of network cooperation is calculated for practicality and scientific cognition of multilayer network structures.

The connections of the lower layer network are created by the Gabriel graph (GG) as the lower layer in our multilayer model (Fig. 3(b)), and the colour of zones corresponds to the population distribution.

We can denote the change of travel costs as the system user's preferred route choices while the network structure is shifting. As a consequence, we denote that

$$\Psi = \frac{\sum \text{SPL} \times w\tau}{\sum \text{SPL}_s \times w\tau} = \sum \frac{U_{ij} w_r \tau_r + L_{ij} w_s \tau_s + C_{ij} w_c \tau_c}{L_{ij} w_s \tau_s} \quad (8)$$

where  $\Psi$  is the ratio of the total travel cost of the total SPL of the network after the rail node is added ( $\sum \text{SPL}$ ) and the total SPL of the lower layer network ( $\sum \text{SPL}_s$  is a constant when other variables are constant),  $w\tau$  is defined as the travel cost per unit distance.

Based on the definition of  $\Psi$  and  $\Lambda$ , we can see that  $\Psi$  is a function of  $\Lambda$ . When the weights of links and the costs of passing through upper and lower layer networks are the same, then we have their relationship function as follows:

$$\Lambda = \frac{C_{ij}}{N(N-1)L_{ij}} \frac{1}{\Psi}. \quad (9)$$

When  $\Lambda$  changes, the  $\Theta$  value has a substantial impact on the choice of the shortest path. As rail station nodes are added, and new lower layer network nodes are generated around them and connected to the network, we can define  $\Psi'$  as the ratio between  $\sum \text{SPL}_{new}$  and  $\sum \text{SPL}_s$ , where  $\sum \text{SPL}_{new}$  is the sum of the SPL of the new network after rail nodes and new

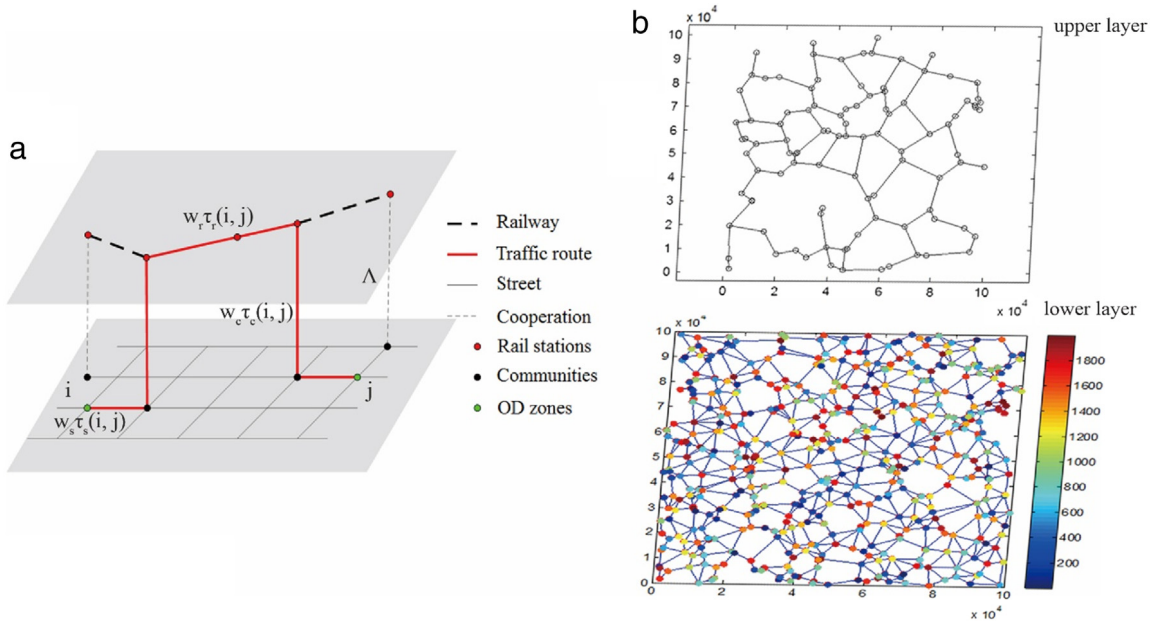


**Fig. 3.** (a) A typical shortest weighted route passes through the upper and lower layers. From zone  $i$  to zone  $j$ , where the red lines are the traffic routes, dark dotted lines on the upper layer are railways, and red points are rail stations. Grey lines on the lower layer are a street line, which connects different zones, and their intersections represent different OD zones (nodes). Grey dotted lines represent the cooperation between different layers. (b) The upper layer is the rail network with 100 rail stations (nodes) with the basic RNG network structure. The lower layer is the initial network with population; the number of nodes is 500, and the colour ranges by the population amount in that node, and its basic network structure is GG. (For interpretation of the references to colour in this figure legend, the reader is referred to the web version of this article.)

lower layer network nodes are added, and  $\sum \text{SPL}_s$  is the sum of SPL of the initial lower layer network. When travel cost is a constant per unit distance, we have:

$$\psi' = \frac{\sum \text{SPL}_{new}}{\sum \text{SPL}_s}, \quad (10)$$

here, we introduce another important indicator representing the uniformity degree of the road network: coverage. It is a basic index used to measure the structure of the road networks and the coverage of the rail station service area. Here, we define coverage as the ratio between the area serviced by the rail station and the entire urban area. This is the intuitive definition of coverage based on the nature of rail networks that service only a limited area around rail stations, unlike the definition in fractal geometry, which uses the lattice method for the division to calculate urban road coverage. Therefore, we have the function of coverage:

$$\text{Coverage} = \frac{\sum \text{rail station service area} - \sum \text{overlapped area}}{\sum \text{urban area}}. \quad (11)$$

Accessibility is a fundamental definition of urban design and transportation planning and has been defined as some measure of spatial separation of human activities, in another word, the collective performance of traffic network and urban land use can be illustrated by this index. For the multilayer system, as a feature of sustainable development expressed regarding quality of life and measured by various indicators, node accessibility  $A$  also can be used to assess the merits of urban network design directly. Hence we treat it as the average level to access a surrounding area with a limited budget. We use the ratio of the travel cost to illustrate the relation when  $\theta$  is in flux. Then we have,

$$A = \frac{N \left| \sum_{w\tau(i,j) < w\tau'} d_{\min}^{ij} \right|}{N^2} \quad (12)$$

where  $N \left| \sum_{w\tau(i,j) < w\tau'} d_{\min}^{ij} \right|$  is the number of nodes that can be reached within a given travel cost  $w\tau'$ , and  $N^2$  is the total number of possible nodes in an adjacent matrix.

Betweenness centrality is widely used to describe the typical structural importance of edges or nodes. When analysing network congestion effects, betweenness centrality can be used to find out which route network transit users are most likely to choose. With the network growing process, we normally represent betweenness centrality using the Gini coefficient,



which also shows that edges with more loaded traffic flow become more critical as the  $\Theta$  is increasing. Here, we define the Gini coefficient of betweenness centrality as proposed by Dixon, Weiner [51], using the following formula:

$$\text{Gini} = \frac{1}{2 \times \overline{BC} \times N \times (N - 1)} \sum_{i=1}^N (2i - N - 1) \times BC_i \quad (13)$$

where  $\overline{BC}$  is the average betweenness centrality of the graph.

#### 2.4. Coevolution approach

Suppose that in a limited area, at the beginning of the expansion of urban rail networks, the population data are randomly distributed to their related nodes, and the transportation of residents follows this allocation pattern. When the travel rate reaches a certain high level, car-based travel cannot satisfy normal transit needs, and this limited traffic capacity triggers traffic congestion. At this point, high efficiency and capability rail transit will appear to alleviate this phenomenon. Here, we can assume that the rail network is set up according to the population distribution; thus, the location of rail transit stations is based on the connection of selected points with the current highest population density or the highest population amounts, which generates a simulated upper layer network.

Here, we face two different situations. The first is when the rail network is growing and the lower network is static. The second is lower network growth accompanied by a growing rail network. The first situation is frequently encountered in limited construction areas or in areas in which there are no construction conditions, such as built-up areas, environmental protection areas and water areas in urban planning. The second situation occurs more commonly. We analyse and discuss these two cases comprehensively.

In the lower network expansion process and generally in parallel with cities' growth, some small communities (nodes) are generated in considering transport efficiency for the purpose of increasing location advantage, improving the convenience of local life and exchanging goods or commutes more easily. These considerations further enhance accessibility and create commercial value for real estate. Moreover, the new nodes will need rail transit sites. In our model, we choose to locate these nodes randomly, in line with the Newman–Gastner model [52]. These advantaged nodes gather more residents from other nodes, and the number of increased population from other nodes is evenly divided and distributed to the new nodes as migration. Later, a new node may generate the highest population and form a coevolution circle. Based on this definition, we have  $V^U \in V^L$ ; therefore, the generated multilayer coevolution network is a coupled random network.

#### 2.5. The choose of basic structures of different layers

According to the planar restriction with no crossing links, this network has sparse characteristics, and refers to the number of neighbour nodes in the generated topology is smaller than a constant. In this context, Minimal Spanning Tree (MST) [53], Relative Neighbour Graph (RNG) [54] and Gabriel Graph (GG) [55] are introduced to describe the accessibility of a network, and used for the construction of planar network topology structures. These graphs are related as  $\text{MST} \subseteq \text{RNG} \subseteq \text{GG}$  [56], generally, the RNG can be created by using distributed algorithm easily, but the accessibility and connectivity are relatively poor than GG [56,57], here we use the network efficiency (EG) to describe the network performance.

For the rail networks, which include subway, light rail, tram, trolley, monorail and maglev etc., the description of their structures by MST is over simplified, based on the purpose of local development and increase the connectivity and accessibility, the rail network will become more complex than one-to-one and the structure loops will generate [26]. Here we use the Kuala Lumpur rail network data since 1995 to 2017 [26] to describe the change of network efficiency (EG) under different network structures, the nodes size of these networks in a specific year is the same (such as in 2017 all these four network structures have 193 nodes, but for the MST, RNG and GG, their value is the average of 100 times simulation), see Fig. 4. We noticed that the general trends of the network EG is decreasing when the network size is increasing; the GG always have most efficient topology structure; when the network size is small (for 1995, only 40 nodes), the EG of the real network is lower than MST, but it increase to close with RNG while the network size growing. With the correlation test, the real network have highest correlation with RNG, then we noticed that the RNG is vivid to depict the upper layer network or rail network, but not for the description of lower layer network, because for the lower layer network there always have more than one connections with its neighbours. Similarly we can make comparison of lower layer network and find out that GG is the more suitable structure. Therefore, we choose the GG to describe the connected network of different zones and use the RNG to describe the connected network of various rail stations.

#### 2.6. Related hypothesis

The following are some of the assumptions made in this research:

- (1) All the weights of different roads' development difficulty and capacity are treated as the same to simplify calculation.
- (2) The growth of the lower layer network is based on the rail network and random growth in a given range (this range can be collected by average rail service radius), and the location of upper layer network is depend on the lower layer network.

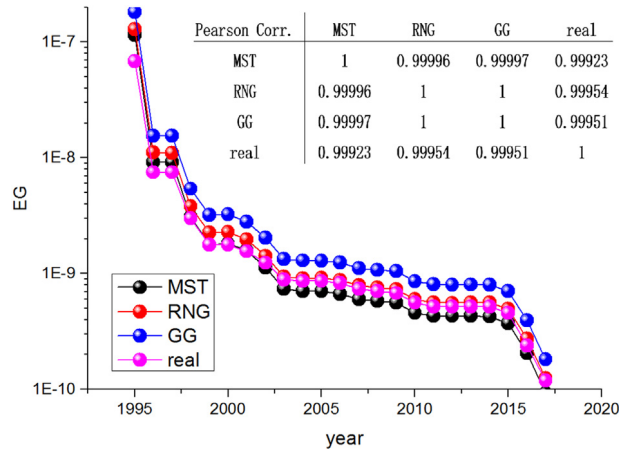


Fig. 4. The EG of the Kuala Lumpur since 1995 to 2017 by different network structures, say the MST, RNG, GG and real.

- (3) We assume that individuals traverse the network using the shortest weighted paths; thus each flow element can easily choose the starting/ending transport mode that might minimize the distance between related zones [37].
- (4) The total network population increases over time due to net migration from other places and natural growth [27].
- (5) The GG is chosen to describe the lower layer network, and the RNG is used to describe the upper layer network.

### 3. Results

We begin the analysis of the coevolution model described in the Methods section. Suppose that an square urban area with length equal to 100 km, denoted the length as  $a = 10 \times 10^4$ , has an initial number of randomly distributed nodes ( $n = 500$ ) with an initial population of 500 thousands and an increasing rate of 1.5% per iteration (include migration) [58].

As we assume in the Methods section, based on residential convenience and the additional commercial value when the population increases, people are often absorbed by newly generated nodes. By sorting the nodes with the highest population, we arrive at the priority node for rail transit development. We connect these nodes using the RNG with 100 iterations representing a rail network as the upper layer. Links connect the same node to different layers, representing the possibility that residents switch between transportation modes in this node easily with a theoretical distance equal to 1. When a rail station is added to the multilayer network, we presume that  $n_{add}$  more nodes will be randomly generated in the lower layer network around the rail station less than about  $dist_{fw}$  km. The value of  $n_{add}$  and distances  $dist_{fw}$  can be set to  $n_{add} = 5$  and  $dist_{fw} = 1000$  (1 km) to simplify the calculations.

In this research, first we need to calculate the population data of the whole city, here the computational complexity is  $O(V)$ , here  $V$  is the number of nodes. Then we calculate the ratio of the total travel cost of the total SPL of the network after the rail node is added ( $\sum SPL$ ) and the total SPL of the lower layer network ( $\sum SPL_s$ ), we use the Dijkstra algorithm (which we know the computational complexity  $O(V^2)$ ) to get the value of  $\sum SPL$  and  $\sum SPL_s$ , hence the computational complexity is  $O(2V^2)$ . On our sparse unweighted graph, calculating betweenness and closeness centrality only takes  $O(|V| |E|)$  time when using Brandes' algorithm [59], here  $E$  is the number of edges. So the computational complexity for the proposed algorithm is  $O(2V^2 + 2 |V| |E|)$  when the number of  $V$  and  $E$  are relatively huge.

When the rail network grows following the population distribution but lower layer network does not change, then we have their clear relationship (Fig. 5(a)). For the multilayer network, when 20 rail stations are added, the average path length (APL) of the multilayer network decrease dramatically nearly 60%. The efficiency global (EG) of the multilayer network increases to its peak and then drops gradually. Above is the depiction of a random multilayer network and its uniformity, features and influence on network structures, including the location of nodes and RNG connections. Here, we must contemplate the general features of networks. When a rail node is added and other variables are constant, the shortest path length (SPL) will change. In addition, the total travel cost of passing through the SPL will change, and a changing trend can be observed by the addition of a rail node to the network.

After 100 iterations denoting an additional 100 rail nodes, we find that, when the upper layer receives approximately 40 nodes, the  $\Psi$  reaches the lowest value (Fig. 5(b)), which indicates that  $\sum SPL$  touches its lowest value after the addition of 40 nodes, where  $\sum SPL_s$  is a constant. Therefore, the structure of a new network is optimized. We can see that it is a good fit by a combined Gaussian function with  $R$ -square = 0.9831:

$$f(x) = a1 * \exp\left(-\left(\frac{x-b1}{c1}\right)^2\right) + a2 * \exp\left(-\left(\frac{x-b2}{c2}\right)^2\right). \quad (14)$$



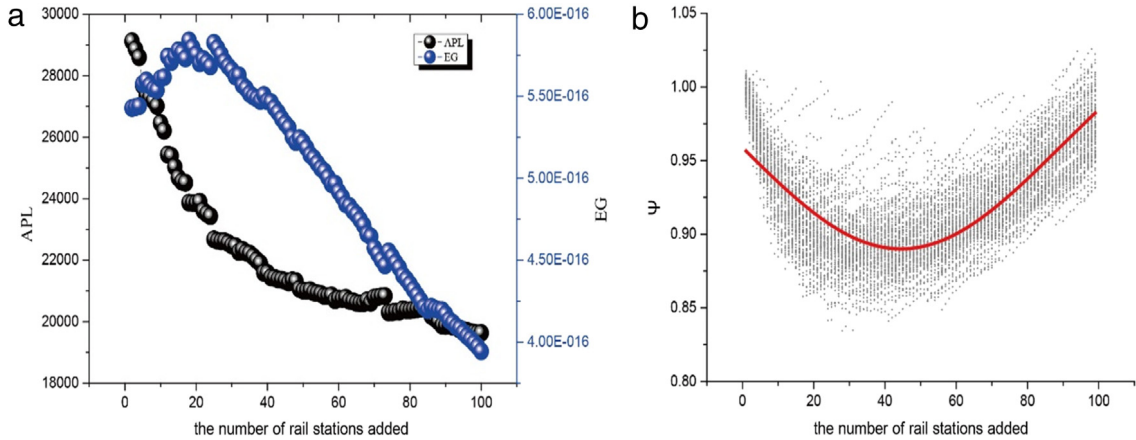


**Fig. 5.** (a) When rail stations are added, the average path length of the multiplex network decreases, and the value of EG has a certain fluctuation. (b) The  $\Psi$  value changes when rail stations are added. It can be better fit by a Gaussian function, where the scaling factors are  $a1 \in [-1.166e + 18, 1.166e + 18]$ ,  $b1 \in [-3.555e + 04, 3.532e + 04]$ ,  $c1 \in [-3113, 3154]$ ,  $a2 \in [-0.501, 2.343]$ ,  $b2 \in [-1.083, 6.442]$ ,  $c2 \in [-3.227, 12.85]$ , here, we choose  $a1 = 1.172e + 14$ ,  $b1 = -117.4$ ,  $c1 = 20.15$ ,  $a2 = 0.9208$ ,  $b2 = 2.68$  and  $c2 = 4.812$ .

The above discussion shows the condition of randomly distributed network nodes with changes in  $\Psi$  during the network growing process. We ignore the multilayer network operation situation; in other words, a change in  $\Theta$  is always accompanied by a different demand on the urban development of the local economy or local rules, and it can be different in different cities, as  $\Theta$  is a variable parameter. Therefore, based on various  $\Theta$  values we find that, in the network evolution process mentioned above,  $\Psi$  has a relatively close relation with  $\Theta$  (Fig. 6(a)). When  $\Theta = 0.01$ , the average travel speed passing through the lower layer network is 1% of the speed via rail network. Adding 20 rail station nodes causes the value of  $\Psi$  to drop close to 60%, but this type of situation is rare, and the speed difference would normally not be that distinct. When the average operation speed on the lower layer network is 1/4 of the speed rate on the upper layer network (the red part in Fig. 5(a)), after 40 station nodes are added, the  $\Psi$  value stabilizes after 40 stations. Meanwhile, when  $\Theta$  is bigger than 0.5, adding rail station nodes will make the  $\Psi$  value increase with iterations, consequently, without considering the traffic jam coefficient and traffic capacity, the distance of passing by rail network from zone  $i$  to zone  $j$  is much longer than the distance via the lower layer network.

When the value of  $\Theta$  is changing, transit users shift between different traffic models to save time or travel costs, the user behaviours are changed. From Fig. 6(b), we can see that when the value of  $\Theta$  changes from 0.001 to 1, the addition of 100 nodes to the network has a huge impact on the APL, particularly when weighted APL is calculated based on the travel cost of networks. Similarly, when  $\Theta = 0.01$ , the APL declines most rapidly; when  $\Theta = 1$ , the APL value takes a horizontal position. In this situation, the addition of rail station nodes has no impact on the general network, i.e., APL. In Fig. 6(c), we can observe that when  $\Theta = 0.25$  and 40 rail station nodes are added, the EG value of the entire network shows an intensifying trend but subsequently shows a gradually declining trend. When  $\Theta = 0.01$ , regardless of how many rail station nodes are added, the influence is positive, which leads to and EG upsurge. Then, we find that the transformation threshold value of  $\Theta$  is between 0.25 and 0.5.

What makes this change so dramatically? When the upper layer network and lower layer network are growing simultaneously, there is a relation between  $\Lambda$  and  $\Theta$ , whereas  $\Lambda$  follows the increase in  $\Theta$  (Fig. 7(a)). Their relation fits the function  $y = Intercept + B1 * x^1 + B2 * x^2 + B3 * x^3$  with  $Adj.R-Square = 0.9939$  as related parameters (see Fig. 7(a)). The interrelation is that  $\Lambda$  reflects user behaviour presented by the shortest weighted path determined by the urban population distribution and urban land use, and  $\Theta$  reflects network operation rules and policies used to adjust the network function layout. The previous definitions show that, considering travel costs, the smaller the  $\Lambda$  value, the higher the network cooperation strength. When the relative speed of the lower layer network decreases, more people use the multilayer system. After analysing the relation between APL and  $\Theta$ , the relation of several other indexes can be observed, such as APL and  $\Lambda$ , after adding 100 rail station nodes. Based on the simulation results shown in Fig. 7(b), we can see that the length of the average shortest path increases as the actual coupling strength of the two layers decreases.

When  $\Theta$  changes from 0.01 to 1 (Fig. 7(c)), the value of  $\Psi'$  changes dramatically. With the increase of  $\Theta$ ,  $\Psi'$  increases from approximately 2.5 to 3.4, which indicates that, the relative speed of the rail system is decreasing when  $\Theta$  is growing. Moreover, the value of  $\Lambda$  is increasing and the APL is thus increasing; thus, fewer people use the rail system, and the layered network degenerates into two separate networks. Closeness centrality (CC) is also measured here by its average value (Fig. 7(d)), as CC is the inverse of the average path length from a given node to other nodes. We can observe that CC has a steadily declining trend when the value  $\Theta$  becomes increscent.

As Fig. 8(a) shows, when the lower layer network is unchanging, we can first reach nearly anywhere in the budget of 30,000 units in travel costs, with assessment of travel cost based on the evaluation of APL. As  $\Theta$  increases by 50%, the value of A decreases sharply by 70%, which indicates that, when the relative speed of street travel increases, cooperation strength

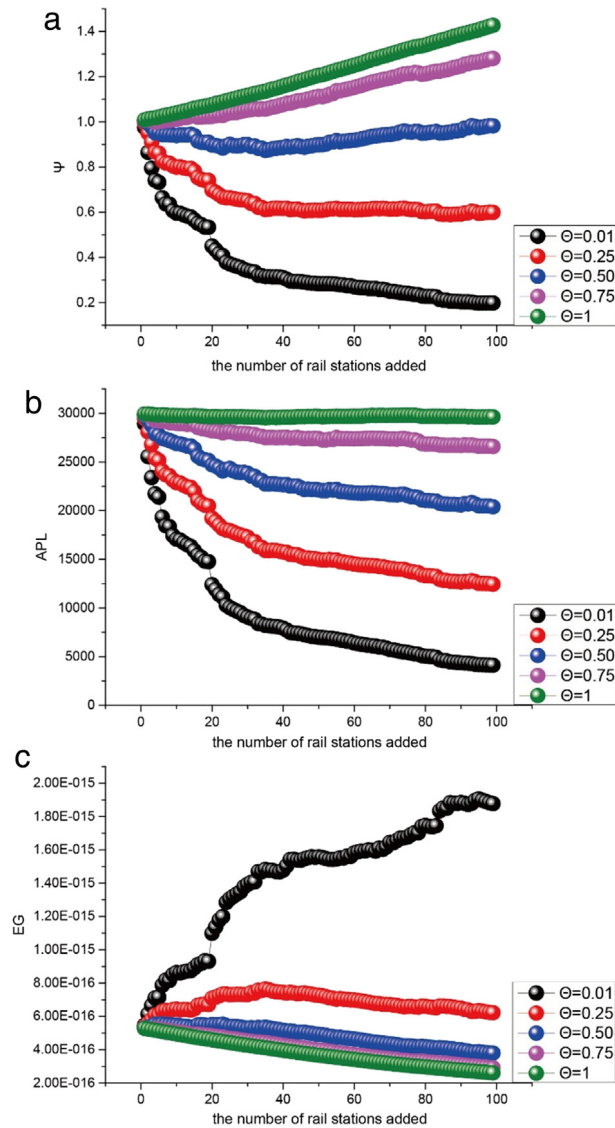


**Fig. 6.** This figure shows that, when 100 nodes are added, the values of  $\Psi$  (a), APL (b) and EG (c) change dramatically as the value of  $\theta$  varies.

declines, and fewer people will use the multilayer system, for their relative distance increases. Thus, the ratio of A drops with a steep slope, which also shows a centralization effect from  $\theta$ . Conversely, in Fig. 8(b), we note that when both layers have a syntrophic relation, i.e., when  $\theta$  is increasing, A is also dropping but relatively flat, even when the average speed of the lower layer network is equal to the mean speed of rail network. In this case, 45% of nodes can still be reached with the given travel cost.

Suppose that the radius of the service area is  $r$ . When 100 nodes are added following the process proposed above and  $r$  is increasing, then we have a logistic equation as shown in Fig. 9(a). Thus, when 100 rail stations are added, we must improve the service radius to 10 km to make the coverage reach 100% and 4 km to 5 km to make the coverage reach 50%. When the service radius is a constant (or 2 km in our simulation in Fig. 9(b)), nearly 500 vertices added to the rail system can cover approximately 50% of the urban area. Considering the random distribution of initial nodes, this rate would be higher in a centralized city.

When the Gini is increasing, the rail transit system aggregates more traffic routes, and the distribution of traffic routes becomes heterogeneous, which also indicates that use of the rail system is becoming more efficient. As  $\Lambda$  is a network structure indicator, based on the relation between  $\theta$  and  $\Lambda$  (Fig. 7(a)), we have the relation between the Gini,  $\theta$  and  $\Lambda$  (Fig. 10). When  $\theta$  is in the 0.7–0.8 interval, the multiplication of the Gini and  $\Lambda$  reach the maximum value, which reflects the network structure's characteristic performances. This finding fits the research of [13]; as their example is a particular case, we can observe that the simulated relation between the Gini,  $\theta$  and  $\Lambda$  has an optimal point for the design of multilayer networks, particularly in the coevolution process.

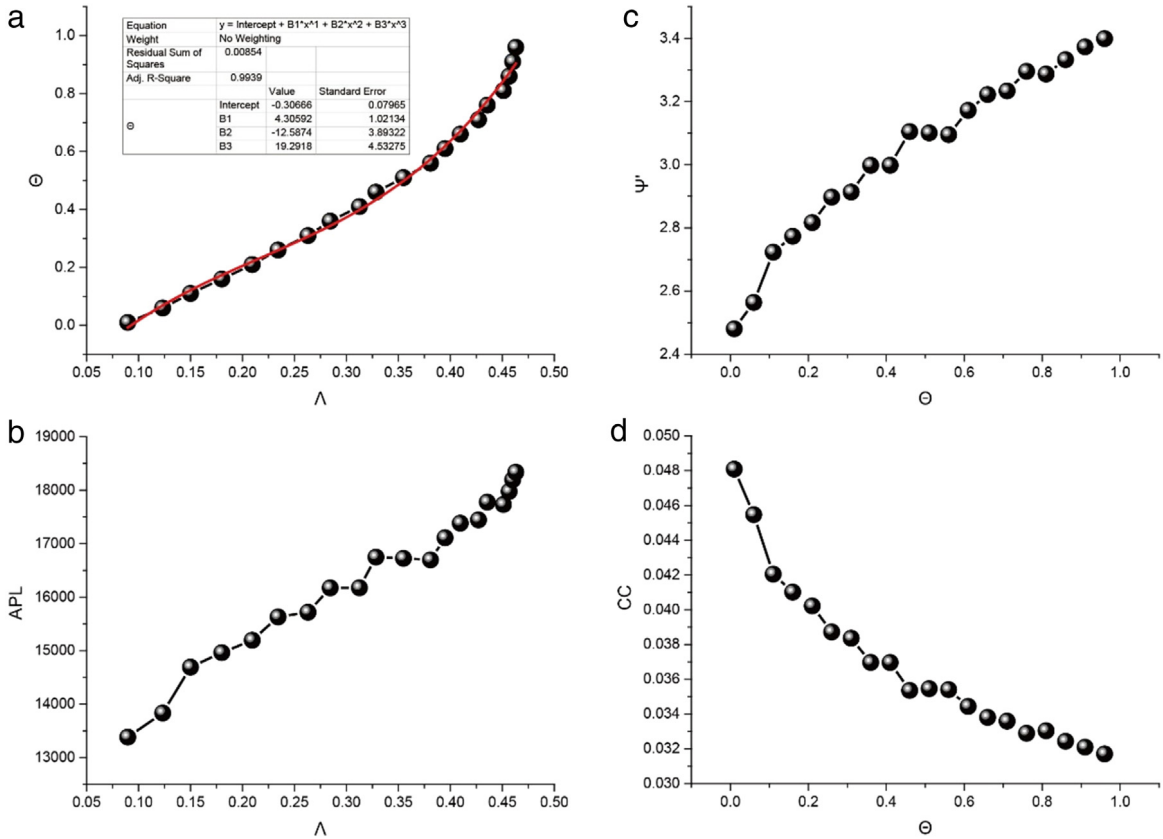


**Fig. 7.** (a) The relation between  $\Delta$  and  $\vartheta$ . The red line is the fit function, and related parameters are shown in the box. (b) The relation between  $\Delta$  and APL. (c) The relation between  $\vartheta$  and  $\psi'$ . (d) The relation between  $\vartheta$  and CC. (For interpretation of the references to colour in this figure legend, the reader is referred to the web version of this article.)

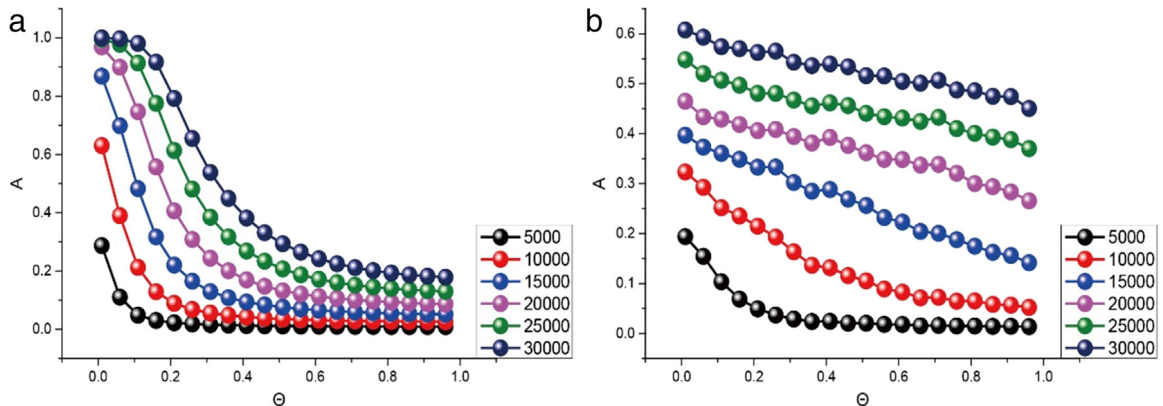


**Fig. 8.** (a) The relation between  $\vartheta$  and A, when the street network is changeless. (b) The relation between  $\vartheta$  and A, when both layers are growing.

#### 4. Conclusion

Multilayer representation of interacting networks can facilitate the explanation and investigation of many systems. Different layers of rail, road, airline and pedestrian networks cooperate and interplay to achieve certain functionalities. In this article, we first introduce RNG and GG to represent the multilayer traffic network, considering the cooperation strength  $\Delta$  and average operation speed ratio in different layers  $\vartheta$  and their impacts on the network structures. Then, based on the network's coevolution process and coupling features, we find that, when the upper layer gains a fixed number of nodes, the  $\psi$  value reaches its lowest value.  $\Delta$  and  $\vartheta$  have a positive relation, and with their cooperation, the value of  $\psi$ ,  $\psi'$ , APL and CC change with positive and negative relations. Accessibility is analysed considering the single layer network's growth and

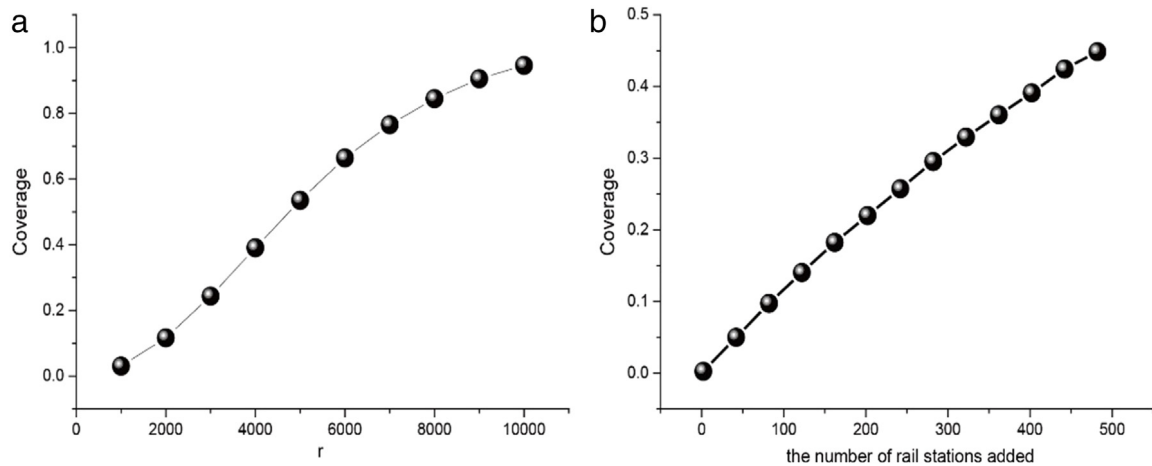


**Fig. 9.** (a) The relation between the coverage ratio and the service area radius. (b) The change trend of coverage by number of rail stations added.

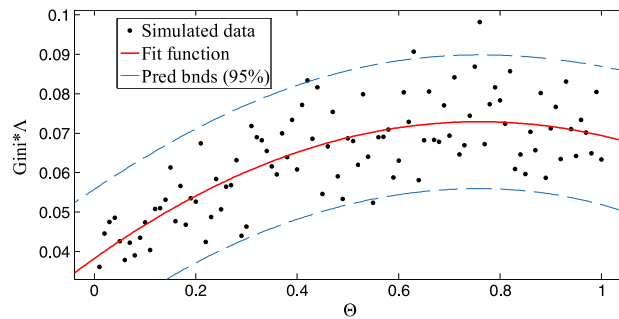


**Fig. 10.** The relation between the Gini,  $\Theta$  and  $\Lambda$ . This graph is simulated by 100 times iterations, where  $n = 100$ , the number of rail nodes added is 20, and other initial conditions do not change. The fit function is  $f(x) = p1 * x^2 + p2 * x + p3$ , where  $p1 = -0.06025$  ( $-0.08281, -0.03769$ ),  $p2 = 0.09145$  ( $0.06793, 0.115$ ),  $p3 = 0.03821$  ( $0.03307, 0.04336$ ), and adjusted  $R$ -square = 0.5852.

the multilayer's coevolution process, with some interesting results. The Gini coefficient of betweenness centrality, which is proposed to imitate the distribution of traffic routes, finds an optimal point.

This research shows that general network design is highly related to the network cooperation strength and future operation speed ratio of different layers and that the maintenance and the better operation of the existing networks also rely on these indicators. With deeper consideration of the cooperation strength, we can make the different traffic layers function better. This research deepens the understanding of their relationships, which is paramount, particularly in the process of urban network design when we want to improve the entire network performance using current network characteristics and user's behaviour change. Looking further to avoid cascading failure, we can determine which part needs more investment and which part has more potential for future development. Although the simulation of lower layer network may include every situations of a city, we still need more data to apply our heuristic method to a real project, and further the optimization process.

## Acknowledgements

## Funding Statement

Financial support came from China National Funds for Distinguished Young Scientists (grant no. 71525002), National Natural Science Foundation of China (grant no. 71621001 and 71271024), Research Foundation of State Key Laboratory of Rail Traffic Control and Safety (grant no. RCS2017ZZ001) and the Fundamental Research Funds for the Central Universities (grant no. 2016JBZ007).

## Data Accessibility

My research is based on the simulation of the urban network coevolution process, so there is no real data. All the simulation data can be found in this paper.

## Competing Interests

We have no competing interests.

## Authors' Contributions

R.D., N.U. and J.W. conceived and designed the research project and interpreted the data. R.D., H.H., M.S.A.M. and R.L. conducted majority of the simulation and the analysis. All authors prepared and finalized the manuscript.

## References

- [1] M.G. Bell, Y. Iida, *Transportation Network Analysis*, 1997.
- [2] R. Guimera, et al., The worldwide air transportation network: Anomalous centrality, community structure, and cities' global roles, *Proc. Natl. Acad. Sci.* 102 (22) (2005) 7794–7799.
- [3] T.L. Friesz, Transportation network equilibrium, design and aggregation: key developments and research opportunities, *Transp. Res. A* 19 (5) (1985) 413–427.
- [4] S. Melkote, M.S. Daskin, An integrated model of facility location and transportation network design, *Transp. Res. A* 35 (6) (2001) 515–538.
- [5] W. Chan, T. Fwa, C. Tan, Road-maintenance planning using genetic algorithms. I: Formulation, *J. Transp. Eng.* 120 (5) (1994) 693–709.
- [6] J. Current, M. Marsh, Multiobjective transportation network design and routing problems: Taxonomy and annotation, *European J. Oper. Res.* 65 (1) (1993) 4–19.
- [7] M. Barthélemy, A. Flammini, Co-evolution of density and topology in a simple model of city formation, *Netw. Spat. Econ.* 9 (3) (2009) 401–425.
- [8] P. Oikonomou, P. Cluzel, Effects of topology on network evolution, *Nat. Phys.* 2 (8) (2006) 532–536.
- [9] X. Franch-Auladell, M. Morillas-Torné, J. Martí-Henneberg, The railway network and the process of population concentration in Spain, 1900–2001, *Rev. Hist. Econ.* 32 (3) (2014) 351–379. *Journal of Iberian and Latin American Economic History*.
- [10] P. Adamidis, V. Petridis, Co-operating populations with different evolution behaviours, in: *Proceedings of IEEE International Conference on Evolutionary Computation*, 1996, IEEE, 1996.
- [11] E.G. Irwin, N.E. Bockstael, Interacting agents, spatial externalities and the evolution of residential land use patterns, *J. Econ. Geogr.* 2 (1) (2002) 31–54.
- [12] F. Jian, Spatial-temporal evolution of urban morphology and land use structure in Hangzhou, *Acta Geograph. Sin.* 3 (2003) 002.
- [13] E. Strano, et al., Multiplex networks in metropolitan areas: generic features and local effects, *J. R. Soc. Interface* 12 (111) (2015) 20150651.
- [14] M. Barthélemy, A. Flammini, Optimal traffic networks, *J. Stat. Mech. Theory Exp.* 2006 (07) (2006) L07002.
- [15] D. Levinson, B. Yerra, Self-organization of surface transportation networks, *Transp. Sci.* 40 (2) (2006) 179–188.
- [16] B.M. Yerra, D.M. Levinson, The emergence of hierarchy in transportation networks, *Ann. Reg. Sci.* 39 (3) (2005) 541–553.
- [17] H. Sun, Z. Gao, J. Wu, A bi-level programming model and solution algorithm for the location of logistics distribution centers, *Appl. Math. Model.* 32 (4) (2008) 610–616.
- [18] J.-J. Wu, Z.-Y. Gao, H.-j. Sun, Optimal traffic networks topology: A complex networks perspective, *Physica A* 387 (4) (2008) 1025–1032.
- [19] Z. Gao, J. Wu, H. Sun, Solution algorithm for the bi-level discrete network design problem, *Transp. Res. B* 39 (6) (2005) 479–495.
- [20] D. Levinson, Density and dispersion: the co-development of land use and rail in London, *J. Econ. Geogr.* (2007) 55–77.
- [21] F. Xie, D. Levinson, Measuring the structure of road networks, *Geograph. Anal.* 39 (3) (2007) 336–356.
- [22] F. Xie, D. Levinson, Topological evolution of surface transportation networks, *Comput. Environ. Urban Syst.* 33 (3) (2009) 211–223.
- [23] F. Xie, D. Levinson, Modeling the growth of transportation networks: a comprehensive review, *Netw. Spat. Econ.* 9 (3) (2009) 291–307.
- [24] J. Wu, M. Xu, Z. Gao, Modeling the coevolution of road expansion and urban traffic growth, *Adv. Complex Syst.* 17 (01) (2014) 1450005.
- [25] T. Li, et al., Integrated co-evolution model of land use and traffic network design, *Netw. Spat. Econ.* (2015) 1–25.
- [26] R. Ding, et al., Complex network theory applied to the growth of Kuala Lumpur's public urban rail transit network, *PLoS One* 10 (10) (2015) e0139961.
- [27] F. Zhao, et al., Population-driven urban road evolution dynamic model, *Netw. Spat. Econ.* (2015) 1–22.
- [28] F. Zhao, et al., Analysis of road network pattern considering population distribution and central business district, *PLoS One* 11 (3) (2016) e0151676.
- [29] F. Zhao, et al., Urban road network evolution to maximize the capacity, *Procedia - Soc. Behav. Sci.* 138 (2014) 251–258.
- [30] Y. Chen, A new model of urban population density indicating latent fractal structure, *Int. J. Urban Sustain. Dev.* 1 (1) (2009) 89–110.
- [31] E. Alvarez, X. Franch, J. Martí-Henneberg, Evolution of the territorial coverage of the railway network and its influence on population growth: The case of England and Wales, 1871–1931, *Hist. Methods: A J. Quant. Interdiscip. Hist.* 46 (3) (2013) 175–191.
- [32] M. Kurant, P. Thiran, Layered complex networks, *Phys. Rev. Lett.* 96 (13) (2006) 138701.
- [33] S.V. Buldyrev, et al., Catastrophic cascade of failures in interdependent networks, *Nature* 464 (7291) (2010) 1025–1028.
- [34] J. Ma, et al., Improved efficient routing strategy on two-layer complex networks, *Internat. J. Modern Phys. C* 27 (4) (2015) 1650044.
- [35] J. Ma, et al., Traffic dynamics on two-layer complex networks with limited delivering capacity, *Physica A* 456 (2016) 281–287.
- [36] J. Ma, et al., Enhancing traffic capacity of scale-free networks by link-directed strategy, *Internat. J. Modern Phys. C* 27 (03) (2016) 1650028.
- [37] A. Solé-Ribalta, S. Gómez, A. Arenas, Congestion induced by the structure of multiplex networks, *Phys. Rev. Lett.* 116 (10) (2016) 108701.
- [38] C.-G. Gu, et al., Onset of cooperation between layered networks, *Phys. Rev. E* 84 (2) (2011) 026101.
- [39] S. Porta, P. Crucitti, V. Latora, The network analysis of urban streets: a primal approach, *Environ. Plann. B: Plann. Des.* 33 (5) (2006) 705–725.
- [40] S. Porta, P. Crucitti, V. Latora, The network analysis of urban streets: a dual approach, *Physica A* 369 (2) (2006) 853–866.
- [41] S. Boccaletti, et al., Complex networks: Structure and dynamics, *Phys. Rep.* 424 (4) (2006) 175–308.
- [42] S. Derrible, C. Kennedy, Applications of graph theory and network science to transit network design, *Transp. Rev.* 31 (4) (2011) 495–519.
- [43] R.G. Morris, M. Barthélemy, Transport on coupled spatial networks, *Phys. Rev. Lett.* 109 (12) (2012) 128703.
- [44] K. Okamoto, W. Chen, X.-Y. Li, Ranking of closeness centrality for large-scale social networks, in: *Frontiers in Algorithmics*, Springer, 2008, pp. 186–195.
- [45] L.C. Freeman, A set of measures of centrality based on betweenness, *Sociometry* (1977) 35–41.
- [46] S. Porta, P. Crucitti, V. Latora, Multiple centrality assessment in Parma: a network analysis of paths and open spaces, *Urban Des. Int.* 13 (1) (2008) 41–50.
- [47] S. Porta, et al., Street centrality and densities of retail and services in Bologna, Italy, *Environ. Plann. B: Plann. Des.* 36 (3) (2009) 450–465.
- [48] P. Crucitti, V. Latora, S. Porta, Centrality in networks of urban streets, *Chaos* 16 (1) (2006) 015113.
- [49] S. Porta, V. Latora, 11 Multiple centrality assessment: mapping centrality in networks of urban spaces, in: *Urban Sustainability Through Environmental Design: Approaches to Time-People-Place Responsive Urban Spaces*, 2007, p. 101.
- [50] S. Porta, et al., Street centrality and the location of economic activities in Barcelona, *Urban Stud.* 49 (7) (2012) 1471–1488.
- [51] P.M. Dixon, et al., Bootstrapping the Gini coefficient of inequality, *Ecology* 68 (5) (1987) 1548–1551.
- [52] M.T. Gastner, M.E. Newman, Shape and efficiency in spatial distribution networks, *J. Stat. Mech. Theory Exp.* 2006 (01) (2006) P01015.
- [53] V. Jarník, O jistém problému minimálním. *Práce Moravské Přírodovědecké, Společnosti* 6 (1930) 57–63.
- [54] P.M. Lankford, Regionalization: theory and alternative algorithms, *Geogr. Anal.* 1 (2) (1969) 196–212.
- [55] K.R. Gabriel, R.R. Sokal, A new statistical approach to geographic variation analysis, *Syst. Biol.* 18 (3) (1969) 259–278.
- [56] L. Gang, Z.M.-T.N. Xin-Zheng, S. Ke, A survey of proximity graphs in wireless networks, *J. Softw.* 4 (2008) 015.
- [57] B. Karp, H.-T. Kung, GPSR: Greedy perimeter stateless routing for wireless networks, in: *Proceedings of the 6th Annual International Conference on Mobile Computing and Networking*, ACM, 2000.
- [58] W. Lutz, W. Sanderson, S. Scherbov, The coming acceleration of global population ageing, *Nature* 451 (7179) (2008) 716–719.
- [59] U. Brandes, A faster algorithm for betweenness centrality\*, *J. Math. Sociol.* 25 (2) (2001) 163–177.